



Contents lists available at *Dergipark*

## Journal of Scientific Reports-A

journal homepage: <https://dergipark.org.tr/tr/pub/jsr-a>



**E-ISSN: 2687-6167**

**Number 62, September 2025**

### **RESEARCH ARTICLE**

*Receive Date: 04.02.2025*

*Accepted Date: 22.07.2025*

# **Study of geometric texture on tensile properties of PLA polymer parts produced by FDM**

**Faik Yılan<sup>a\*</sup>, Ibrahim M. M. Alzraiqi<sup>b</sup>, and Levent Urtekin<sup>c</sup>**

<sup>a</sup> *Kırşehir Ahi Evran University, Faculty of Engineering and Architecture, Department of Mechanical Engineering, Kırşehir 40100 Turkey,*  
*ORCID: 0000-0001-7166-8604*

<sup>b</sup> *Kırşehir Ahi Evran University, Faculty of Engineering and Architecture, Department of Mechanical Engineering, Kırşehir 40100 Turkey,*  
*ORCID: 0009-0002-9630-0587*

<sup>c</sup> *Kırşehir Ahi Evran University, Faculty of Engineering and Architecture, Department of Mechanical Engineering, Kırşehir 40100 Turkey,*  
*ORCID: 0000-0003-4348-4749*

---

### **Abstract**

In this study, it is aimed to analyse the effects of texture geometries on mechanical response of polylactic acid (PLA) parts manufactured through fused deposition modeling (FDM). Experimental mechanical analyses of PLA samples with hexagonal, circular, square, full, triangle and ellipse geometries were carried out and their tensile responses were examined. Result show that the full geometry exhibited that the full geometry exhibited the highest tensile strength (36 MPa) and deformation capacity (3.1%), making it ideal for applications requiring maximum load-bearing capacity. However, the elliptical geometry demonstrated strength (28 MPa) and deformation capacities close to the full structure, offering a practical balance between mechanical performance, material savings, and production efficiency. Other geometries, such as hexagonal, circular, and square, provided moderate performance suitable for lightweight designs. X-ray tomography was used to analyse internal structures, manufacturing quality, further supporting the correlation between geometric design and mechanical properties. These findings highlight the potential for optimizing material usage and production time without significantly compromising mechanical performance in 3D-printed PLA components.

© 2023 DPU All rights reserved.

---

\* Corresponding author. Tel.: +90 386 280 2326  
E-mail address: faik.yilan@ahievran.edu.tr

**Keywords:** Fused deposition modeling; Texture geometries; X-ray tomography; Tensile properties; PLA.

---

## 1. Introduction

Additive manufacturing (AM) is a production method that has become widespread in the industry with the development of technology. This technique is essentially the process of completing the production by adding the materials layer by layer to a surface called the production plate using three-dimensional (3D) geometric data [1], [2]. We can list the production types of AM technique for processing different materials as the following:

- Stereolithography (SLA).
- Selective laser sintering (SLS).
- Fused deposition modeling (FDM) [3].

This technique was discovered in 1980s. Since these discovered process were not very efficient at that time, they started to be widely used only in the 2000s. This production method, which has been further developed day by day, has now become very popular in mass production.

In the FDM technique, thermoplastic materials Acrylonitrile Butadiene Styrene (ABS), Polyurethane (TPU) and Poly Lactic Acid (PLA) that are wound on a reel are used as production raw materials [4], [5]. These printer devices operate by controlling several drive elements. A drive unit connected to the reel during production separates the material from the reel as needed. The separated material comes to the feeder of the heater nozzle and is melted there. The molten plastic passing through the fine-tipped channels in the extrusion head is plastered to the production surface as a thin layer and layers are formed. As soon as the plastering process is done, the molten material solidifies. After the first layer, the building layer goes down as much as the layer size and the new step is started. The machine ends the production by renewing this process at each step [6], [7], [8].

Solid models that are planned to be produced often cannot be sent directly to the fabrication device. As a pre-process, the 3D solid model is converted to a file with the STL extension, which is the additive manufacturing standard interface [9]. This STL file makes some adjustments such as error checking, placing support elements where necessary, determining the direction of construction and selecting some device parameters through the intermediate applications suggested by the machine to be produced. This intermediate application then slices the solid model into equal segments, breaking it into two-dimensional (2D) layers. The device that will make the production performs the production process by using the data of these 2D layers [10], [11], [12].

Different texture-patterned geometries produced by the FDM process affect the mechanical properties of the parts [13], [14]. One of early studies was researched by Tonsilav Galeta et al. [15] and they designed the internal structures of the samples as full, honeycombs, drills and stripes and observed the highest tensile strength in the honeycomb model. LR Lopez et al. [16] was 3D printed with smooth and zebra pattern border interface transitions using PLA, TPU and PET filaments. In this case, they revealed that zebra patterned samples showed a decrease in tensile strength and modulus of elasticity. In a different comparative study, S. Batai and M.H. Ali [17] designed honeycomb, pentagonal, square and drill model ABS and PLA specimens with the same volume ratio and optimized their mechanical analysis in the finite element method (FEM). Also, in another study is that changing their geometric structure affects the yield strength of printed parts. Therefore, it was concluded that the hexagonal pattern showed better mechanical properties than the other patterns [18].

The demands for the evaluation and inspection of complex additive manufacturing parts using X-ray technology has gained much importance in recent years [19], [20], [21]. Since X-ray tomography method is a non-destructive scanning, it can be used for analysis in different fields such as industrial and academic [22], [23], [24]. Thanks to X-ray CT, the dimensional evaluation, roughness analysis, density measurement and defect detection of the parts produced with 3D printing technology can be characterized. Thus, X-ray CT offers many advantages such as energy,

material and time savings [25].

As mentioned above, different geometries designs are highly influence on the mechanical properties in 3D printing. In this context, this study aimed to determine the influences of geometries textures (circular, square, elliptical, hexagonal and triangular) with 3D printer parameters on the mechanical properties of PLA filament material. X-ray tomography device was used to check the dimensions, pores and defects of the printed parts.

## 2. Materials and methods

### 2.1. Manufacturing of Specimens and Printing Parameters

In this study specimens were fabricated using a 3D FDM device that was designed and manufactured in-house [14]. Table 1 shows the mechanical properties of PLA (esun3d-Ø1,75 mm). It is considered to analyze PLA filament material that used be commonly used for 3D printing. Table 2 shows the parameter values that are used in 3D printing.

Table 1. Mechanical properties of PLA.

Density (g/cm <sup>3</sup> )	Tensile Ultimate Strength (MPa)	Tensile Yield Strength (MPa)	Young's Modulus (MPa)
1.24	59	70	3500

Table 2. Setup parameters for each sample used in this study.

Parameters	Values
Layer height (mm)	0.2
Extruder temperature (°C)	205
Bed temperature (°C)	45
Print speed (mm/s)	35
Infill density (%)	100
Infill pattern	Line
Print core (nozzle) size (mm)	AA 0.4

There is a specific standard focusing on the tensile testing of polymer materials. Therefore, the dimensions of the specimens were prepared separately in accordance with the ASTM D638 IV standards [26]. Therefore, the specimens with different surface patterns were designed with SolidWorks 2020 software. Holes in different shapes, such as circular, square, ellipse, hexagonal and triangular, were drilled corresponding to the regions of the specimens that were expected to rupture. In order to find out the effect on tensile strength of patterns shape, all specimens have the same number of textures, same area density, and same area of a pattern, as it can be seen Table 3.

Table 3. An example of a table. Design parameters of tensile test specimens.

Pattern geometry	Area density (%)	Number of patterns	Distance of patterns (mm)	Area of a dimple (mm <sup>2</sup> )
Full	100	-	-	-
				
Circle	80	8	4	4.9
				

Square	80	8	4	4.9
				
Ellipse	80	8	4	4.9
				
Hexagon	80	8	4	4.9
				
Triangle	80	8	4	4.9
				

## 2.2. Tensile Tests

Tensile tests were conducted by using a universal testing machine (WDM-100E Model/Japan). The maximum load capacity of the machine was 100 kN. The specimens were carefully clamped in the holders and tensile tests were performed (Fig. 1). Deformation and load data were automatically recorded in a computer system. The test speed was kept as 1 mm/min for all the specimens as suggested by the test standard. Each test was repeated at least five times and tensile strengths of the polymer materials were obtained from the average strengths.



Fig. 1. Overview of the tensile test machine (KAEU-Mechanical Engineering Mechanics Lab.).

### 2.3. X-Ray Tomography

A laboratory scale, an X-CT system generally includes an X-ray source that converts electrical power into X-rays, a rotating stage where the specimen is positioned for scanning, and a detector, as depicted in Fig. 2 (a-b). The main principle of the X-Ray tomography system is related to irradiating the X-ray beam onto the sample and mathematically measuring the images with the help of a detector [27]. YXLON X-Ray tomography unit was used to examine dimensions, pores and defects of the printed samples. The image analysis was performed using at 85 kW and 0.05 A.

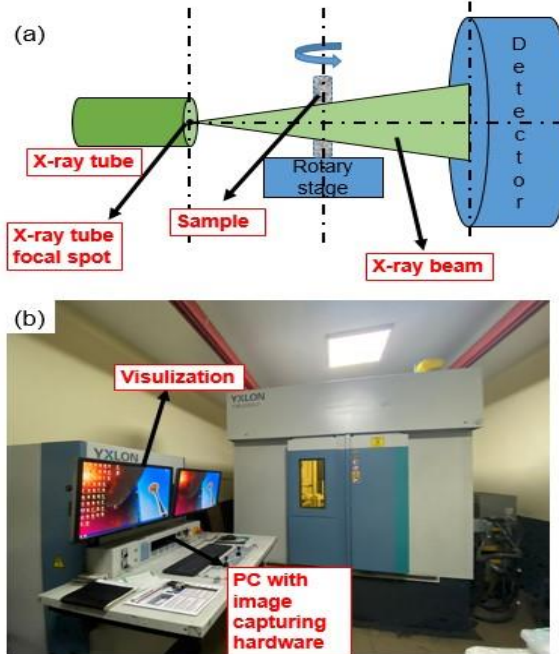


Fig. 2. (a) CT working principle; (b) X-ray computed tomography device.

### 3. Results and Discussion

The Fig. 3 shows a comprehensive analysis of the mechanical performance and stress-strain curves of the PLA material produced from the 3D printer in different geometric textures. The Full structure stands out with the highest tensile strength (36 MPa) and the largest deformation capacity (3.1%) among all geometries. This structure was provided a design where the load-carrying capacity is maximized throughout the entire structure thanks to its continuous and homogeneous internal structure. The Full structure, which exhibits the best performance in terms of strength and deformation, is ideal for applications where heavy loads need to be carried and durability is critical. However, high material usage and weight may make this structure disadvantageous in lightened design requirements. The Ellipse structure draws attention with its strength values (28 MPa) and deformation capacities close to the Full structure (3.1% strain). Although the concave form of the ellipse cannot increase the strength to the Full level, it stands out as a structure that offers sufficient strength and material savings together. Hexagon offers a medium-class mechanical performance with a tensile strength of approximately 25 MPa and a strain capacity of 2.66%. However, the interrupted areas and internal geometric gaps in this structure cause the strength to be lower compared to Full or

Ellipse. Hexagon can be used in medium-load capacity applications where a lightweight structure is required. Circle and Hexagon textures are similar to each other in terms of strength (25 MPa) and deformation capacity (2.75%) and perform at the same limits as the Square structure. Circle has a slight advantage over Hexagon in terms of deformation (3.2% strain) thanks to the uniform distribution of stress. However, both structures exhibit less strength compared to Full and Ellipse textures. These two structures can be preferred in applications where lightness is required and medium load carrying capacity is needed. Triangle offers the lowest strength (22 MPa) and deformation capacity (1.75% strain) among all textures. The sharp angles and corners of the triangular form cause the stress concentration to accumulate in certain areas, accelerating the fracture. Therefore, the Triangle texture is only suitable for designs with low load-carrying requirements and where lightness and aesthetic requirements are more important than durability. Its use is not recommended in areas where strength and durability are priorities.

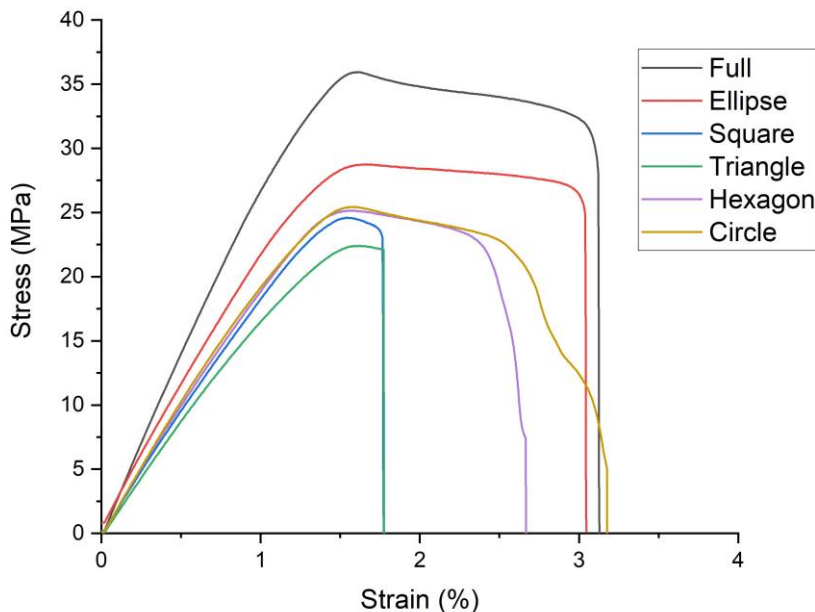


Fig. 3. Tensile stress-strain curve of PLA parts.

In Fig. 4, the tensile strength results show that there is a strong correlation between the design geometry and material performance under tensile stress. The full cross-section, having no stress-concentrating edges or interruptions, understandably achieves the highest tensile strength (36 MPa). This makes it the most reliable structure for applications requiring maximum load-bearing capabilities. On the other hand, shapes with angular edges, such as the square (24 MPa) and triangle (22 MPa), show the lowest tensile strength. This weakness is attributed to stress concentrations at the sharp corners, which reduce their ability to handle uniform tensile forces. Rounded geometries, such as the circle (25 MPa) and ellipse (28 MPa), perform significantly better because they distribute stress more evenly. The hexagon (25 MPa) also achieves decent performance, reflecting its relatively uniform design, though it does not match the strength of smoother, curved shapes.

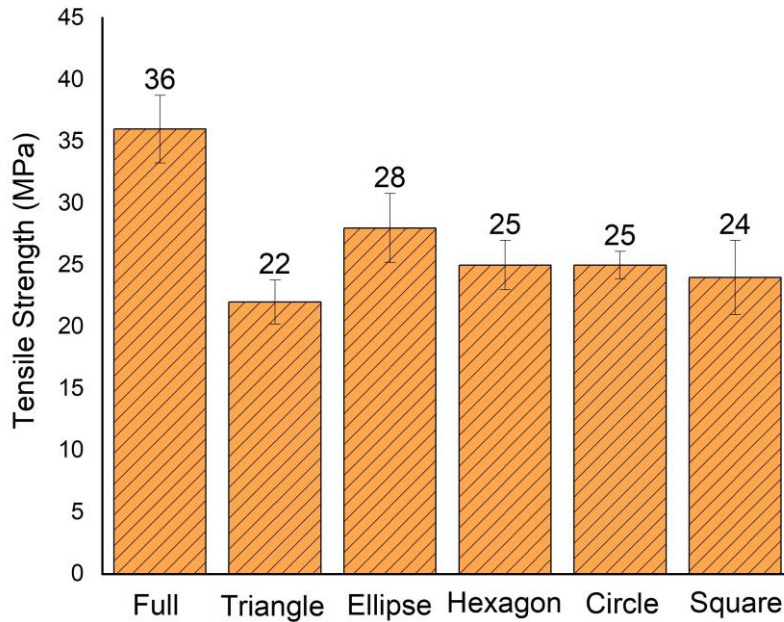


Fig. 4. Results of tensile strength tests.

This X-ray analysis reveals the fundamental differences in the internal structures of different geometric textures produced with PLA material, and these differences allow us to understand the mechanical performance of each structure. The Fig. 5 shows the void shapes, fullness ratios and regularities of the textures, which are critical elements that determine how stress is distributed throughout the material and how it affects behaviors such as fracture or deformation. The full structure has a completely full and homogeneous internal structure. Since there is no void inside, this structure can distribute stress evenly throughout the material and stands out as the most resistant geometry against external effects. This makes the full structure the most robust design, but it also makes it unsuitable for applications that require lightness. The full structure minimizes the risk of sudden breakage thanks to the absence of voids and offers a highly durable integrity. The interior of the ellipse structure is designed with regular and soft oval voids. The elliptical shape enables more uniform stress distribution evenly and reduces the risk of cracking not having any corners or sharp edges. The ellipse design is a balanced option that optimizes weight instead of fullness, while still offering a highly robust performance. A special advantage of this structure is that it offers a balance between lightness and strength. While the Hexagon structure consists of regular hexagonal spaces, the sharp edges of these spaces attract attention. Sharp edges cause stress to accumulate in certain focuses during loading, making the material vulnerable to damage earlier than other regular structures. However, the hexagonal geometry is advantageous in terms of providing lightness and optimizing the fullness ratio. However, this design cannot fully maximize durability and remains at a certain limit. Circle and Square structures generally exhibit similar structural characteristics. While the circular structure can distribute the stress more evenly thanks to its soft edges, the square structure has sharp corners and this increases the risk of breakage. While the circular design provides more balanced strength, the square structure is more

disadvantageous due to sharper geometric focuses. Both structures are suitable for applications that target a mid-range performance between lightness and strength. The triangle structure has the most sharp edges and irregular stress distribution among the analyzed geometries. The sharp edges and corners created by triangles cause stress to concentrate at specific points, resulting in premature fractures. The complexity and discontinuity of its internal structure proves that the triangular design is poor in terms of durability. Although it can be used for light and aesthetic designs, it is not a suitable structure for applications requiring load carrying. This X-ray analysis clearly shows the influence of the internal layouts of geometric structures on the performance of the material. Fully-filled structures offer the highest durability, while structures with regular gaps optimize lightness and minimize weaknesses. While stress is distributed more appropriately in oval and circular structures, weak points occur due to stress accumulation in designs with angular and sharp lines (Triangle and Square).

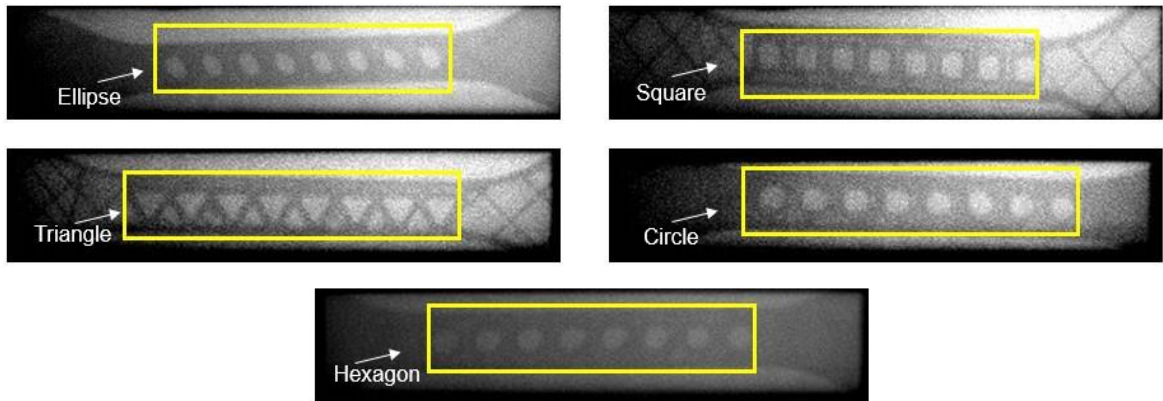


Fig. 5. X-ray images of the PLA parts.

#### 4. Conclusions

This study analyzed the effects of geometric textures on the tensile properties of PLA parts produced using fused deposition modeling (FDM). The results demonstrated that the "Full" geometry exhibited the highest tensile strength (36 MPa) and deformation capacity (3.1%), making it the most suitable design for applications requiring maximum load-bearing capacity and durability. Its continuous and homogeneous internal structure ensures even stress distribution and minimizes weak points, resulting in superior mechanical performance. The elliptical geometry, with strength values (28 MPa) and deformation capacities close to the full structure, offers a balanced solution for applications prioritizing both material savings and mechanical performance. Geometries such as hexagonal, circular, and square exhibited moderate tensile strength and strain capacities, making them suitable for lightweight designs with medium load requirements. The triangular geometry, with the lowest tensile strength (22 MPa), is limited to aesthetic or low-load applications due to stress concentrations at sharp corners. X-ray tomography analysis provided critical insights into the internal structures, dimensions, and defects of the printed samples, highlighting the correlation between geometric design and mechanical properties. These findings emphasize the importance of texture geometry in optimizing the mechanical performance of 3D-printed PLA components.

Future studies could explore the effects of different materials, printing parameters, and more complex geometric patterns to further enhance the mechanical performance and broaden the application scope of FDM technology.

## Acknowledgements

This study was supported by the TUBITAK 2209-A National Undergraduate Student Research Projects Support Programme (Project no: 1919B012319180).

## Author Contributions

F.Y. and I.A. organized and performed all the analyses and wrote the manuscript. L.U. determined the main idea of the study and carried out paper revisions.

## References

- [1] N. Babacan, and H. Seremet, "Investigation of the Load-Bearing Capacity of Co-Cr Lattice Structures Fabricated by Selective Laser Melting," *Int. J. 3D Print. Technol. Digit. Ind.*, vol. 6, no. 2, pp. 286–291, 2022, doi: 10.46519/ij3dptdi.1139802.
- [2] F. Yilan, R. Ekici, and L. Urtekin, "Recent advances in the AlSi10Mg materials fabrication by selective laser melting: process parameters, optimization, low-velocity and ballistic impact responses," *Prog. Addit. Manuf.*, no. 0123456789, 2024, doi: 10.1007/s40964-024-00856-x.
- [3] T. C. Yang and C. H. Yeh, "Morphology and mechanical properties of 3D printed wood fiber/polylactic acid composite parts using Fused Deposition Modeling (FDM): The effects of printing speed," *Polymers (Basel.)*, vol. 12, no. 6, p. 1334, 2020, doi: 10.3390/POLYMI2061334.
- [4] M. Samykano, S. K. Selvamani, K. Kadrigama, W. K. Ngu, G. Kanagaraj, and K. Sudhakar, "Mechanical property of FDM printed ABS: influence of printing parameters," *Int. J. Adv. Manuf. Technol.*, vol. 102, no. 9–12, pp. 2779–2796, 2019, doi: 10.1007/s00170-019-03313-0.
- [5] M. Srivastava, S. Rathee, V. Patel, A. Kumar, and P. G. Koppad, "A review of various materials for additive manufacturing: Recent trends and processing issues," *J. Mater. Res. Technol.*, vol. 21, pp. 2612–2641, 2022, doi: 10.1016/j.jmrt.2022.10.015.
- [6] F. Yilan, İ. B. Şahin, F. Koç, and L. Urtekin, "The Effects of Different Process Parameters of PLA+ on Tensile Strengths in 3D Printer Produced by Fused Deposition Modeling," *El-Cezeri J. Sci. Eng.*, vol. 10, no. 1, pp. 160–173, 2023, doi: 10.31202/cejse.1179492.
- [7] U. L. Yilan, F. Şahin, İ. B., "3d Printing Design and Manufacturing: Dual-Extrusion System," in *New Trends in Engineering Sciences*, New Trends in Engineering Sciences, 2022, pp. 151–161. [Online]. Available: <https://www.dosyaupload.com/3sNvc?pt=VTFKS2VqWIZObTh6TkRSelRXSnNza0p0VHpaeVFUMDIpc29yeTVtaHZQd0YyUkNxMmJNWTY4TT0%3D>
- [8] S. A. M. Tofail, E. P. Koumoulos, A. Bandyopadhyay, S. Bose, L. O'Donoghue, and C. Charitidis, "Additive manufacturing: scientific and technological challenges, market uptake and opportunities," *Mater. Today*, vol. 21, no. 1, pp. 22–37, 2018, doi: 10.1016/j.mattod.2017.07.001.
- [9] P. Cătălin Iancu, E. Daniela Iancu, and D. Alin Stăncioiu, "From CAD Model To 3D Print Via 'STL' File Format," *Fiability Durab.*, no. 1, pp. 73–80, 2010.
- [10] A. Çelebi, and M. M. İmanç, "Evaluation of Mechanical Properties of PLA Auxetic Structures Produced by Additive Manufacturing," *J. Mater. Mechatronics A*, vol. 4, no. 2, pp. 384–396, 2023, doi: 10.55546/jmm.1309858.
- [11] A. Çelebi, A. Korkmaz, T. Yılmaz, and H. Tosun, "3 Boyutlu Yazıcı ile 6 Eksenli Robot Kol Tasarım Ve İmalatı," *Int. J. 3D Print. Technol. Digit. Ind.*, vol. 3, no. 3, pp. 269–278, 2019.
- [12] A. Çelebi and A. Tosun, "Application And Comparison Of Topology Optimization For Additive Manufacturing And Machining Methods," *Int. J. 3D Print. Tech. Dig. Ind.*, vol. 5, no. 3, pp. 676–691, 2021, doi: 10.46519/ij3dptdi.
- [13] P. Zhang and A. C. To, "Transversely isotropic hyperelastic-viscoplastic model for glassy polymers with application to additive manufactured photopolymers," *Int. J. Plast.*, vol. 80, pp. 56–74, 2016, doi: 10.1016/j.ijplas.2015.12.012.
- [14] Y. Kim, Y. Kim, T. I. Lee, T. S. Kim, and S. Ryu, "An extended analytic model for the elastic properties of platelet-staggered composites and its application to 3D printed structures," *Compos. Struct.*, vol. 189, no. January, pp. 27–36, 2018, doi: 10.1016/j.compstruct.2018.01.038.
- [15] T. Galeta, P. Raos, J. Stojšić, and I. Pakši, "Influence of structure on mechanical properties of 3D printed objects," *Procedia Eng.*, vol. 149, no. June, pp. 100–104, 2016, doi: 10.1016/j.proeng.2016.06.644.
- [16] L. R. Lopes, A. F. Silva, and O. S. Carneiro, "Multi-material 3D printing: The relevance of materials affinity on the boundary interface performance," *Addit. Manuf.*, vol. 23, no. June, pp. 45–52, 2018, doi: 10.1016/j.addma.2018.06.027.
- [17] M. H. A. Shaheidula Batai, "Mechanical Performance Optimization of 3D Printing Material," in *Advances in Materials and Manufacturing Engineering*, 2020, pp. 257–263. doi: 10.1007/978-981-15-1307-7\_28.
- [18] S. Ganeshkumar *et al.*, "Investigation of Tensile Properties of Different Infill Pattern Structures of 3D-Printed PLA Polymers: Analysis and Validation Using Finite Element Analysis in ANSYS," *Materials (Basel.)*, vol. 15, no. 15, 2022, doi: 10.3390/ma15155142.
- [19] A. Du Plessis, I. Yadroitsev, I. Yadroitseva, and S. G. Le Roux, "X-Ray Microcomputed Tomography in Additive Manufacturing: A Review of the Current Technology and Applications," *3D Print. Addit. Manuf.*, vol. 5, no. 3, pp. 227–247, 2018, doi: 10.1089/3dp.2018.0060.
- [20] H. Villarraga-g and N. Carolina, "Role of X-ray / CT Technologies in the " 3D Printing Revolution "," no. June, 2017.
- [21] A. du Plessis, "X-ray tomography for the advancement of laser powder bed fusion additive manufacturing," *J. Microsc.*, vol. 285, no. 3, pp. 121–130, 2022, doi: 10.1111/jmi.12930.
- [22] A. du Plessis, S. G. le Roux, and M. Tshibalanganda, "Advancing X-ray micro computed tomography in Africa: Going far, together," *Sci. African*, vol. 3, p. e00061, 2019, doi: 10.1016/j.sciaf.2019.e00061.

- [23] L. Urtekin, F. Bozkurt, and M. Çanlı, “Analysis of biomedical titanium implant green parts by X-Ray tomography,” *J. Mater. Res. Technol.*, vol. 14, pp. 277–286, 2021, doi: 10.1016/j.jmrt.2021.06.083.
- [24] A. du Plessis, I. Yadroitseva, and I. Yadroitsev, “Effects of defects on mechanical properties in metal additive manufacturing: A review focusing on X-ray tomography insights,” *Mater. Des.*, vol. 187, p. 108385, 2020, doi: 10.1016/j.matdes.2019.108385.
- [25] M. R. Khosravani and T. Reinicke, “On the Use of X-ray Computed Tomography in Assessment of 3D-Printed Components,” *J. Nondestruct. Eval.*, vol. 39, no. 4, 2020, doi: 10.1007/s10921-020-00721-1.
- [26] J. J. Laureto and J. M. Pearce, “Anisotropic mechanical property variance between ASTM D638-14 type i and type iv fused filament fabricated specimens,” *Polym. Test.*, vol. 68, no. April, pp. 294–301, 2018, doi: 10.1016/j.polymertesting.2018.04.029.
- [27] F. Dababneh and H. Taheri, “Investigation of the influence of process interruption on mechanical properties of metal additive manufacturing parts,” *CIRP J. Manuf. Sci. Technol.*, vol. 38, pp. 706–716, 2022, doi: 10.1016/j.cirpj.2022.06.008.